Available online at www.sciencedirect.com
SCIENCE DIRECT®
Journal of Power Sources 124 (2003) 118–123
JOURNAL OF POWER SOURCES
www.elsevier.com/locate/jpowsour

$LiCoO_2$ sub-microns particles obtained from micro-precipitation in molten stearic acid

S.M. Lala, L.A. Montoro, J.M. Rosolen*

Department of Chemistry, FFCLRP-University of São Paulo, Avenida Bandeirantes, 14040-901 Ribeirão Preto-SP, Brazil

Received 5 April 2003; accepted 30 April 2003

Abstract

The present work reports a novel emulsion method for preparation of lithium cobalt oxide based on the micro-precipitation of lithium and cobalt salts in molten stearic acid. The precursors consist of micro-aggregated powders of CoOOH and $CH_3(CH_2)_{16}COOLi$ whose formation depends on the concentration of stearic acid used in the synthesis. The micro-aggregated of CoOOH and $CH_3(CH_2)_{16}COOLi$ when calcined at 800 °C yielded well-crystalline sub-microns particles of $LiCoO_2$ (*R*-3*m*) with a very uniform shape (quasi-hexagonal pellets), a very narrow grain size distribution ($d_{10} = 0.31$, $d_{50} = 3.14$, $d_{90} = 6.30\,\mu m$) and high specific surface area ($7.4\,m^2\,g^{-1}$). The long life reversible specific capacity of the mp-$LiCoO_2$ composite electrode subsequently made was $110\,mAh\,g^{-1}$ for initial deinsertion $165\,mAh\,g^{-1}$.

Keywords: Li-ion battery; Oxides; Emulsion

1. Introduction

The preparation of Li-oxide materials is very important for the development of batteries based in lithium intercalation. The synthesis method has a decisive role in the definition of the grain size distribution, porosity distribution, aggregation and morphology of the Li-oxide particles, which influences the lithium electro-intercalation. For example, capacity fading of composite electrodes is associated with loss of ohmic contact in the electrode during lithium intercalation reactions. This mechanical stress and the lithium diffusion have a large influence in the electrochemical performance of electrode and depends on grain size distribution, porosity distribution, aggregation and shape of the Li-oxides particles [1,2]. This explains why it is important to study Li-oxide preparation routes. The main representative example of these oxides is $LiCoO_2$, a compound that can be prepared with several kinds of precursors obtained from lithium nitrate, carbonate, acetate or hydroxide associated or not with a chelating agent. [3–27].

This paper reports a new approach to preparation of Li-oxides: micro-precipitation in molten stearic acid. In this new methodology, an emulsion-derived powder from reaction between molten stearic acid and lithium, cobalt nitrates is prepared. The material chosen for investigation was the well-known $LiCoO_2$. The use of emulsions in preparations of materials can be considered as a soft chemistry method that can be very appropriate to prepare uniform particles. In emulsion methods, the precursor materials are isolated in a phase often liquid or polymeric, as droplets or islands, which acts as independent reactors. The island or droplet dimensions are controlled by the dispersion technique. These features explain why emulsion methods are able, in principle, to provide often homogeneous or monophasic materials with narrow grain size distribution in the sub-micron range determined by the dimension of the precursor particles [26]. In the method discussed here, these islands are the micro-precipitate consisting mainly of mixtures of $CH_3(CH_2)_{16}COOLi$ and CoOOH particles.

2. Experimental

Fig. 1 shows the protocol used in preparation of the $LiCoO_2$ precursor powder. The lithium and cobalt salts ($LiNO_3$, $Co(NO_3)_2{\cdot}6H_2O$, Fluka) were initially mixed in a mortar and then added to molten stearic acid (Reagen) at 90 °C (molar proportion metal/acid 1:1 or 2:1). This mixture was then submitted to vigorous magnetic stirring at

* Corresponding author. Tel.: +55-16-602-3787; fax: +55-16-633-8151.
E-mail address: rosolen@ffclrp.usp.br (J.M. Rosolen).

0378-7753/$ – see front matter © 2003 Elsevier B.V. All rights reserved.
doi:10.1016/S0378-7753(03)00615-3

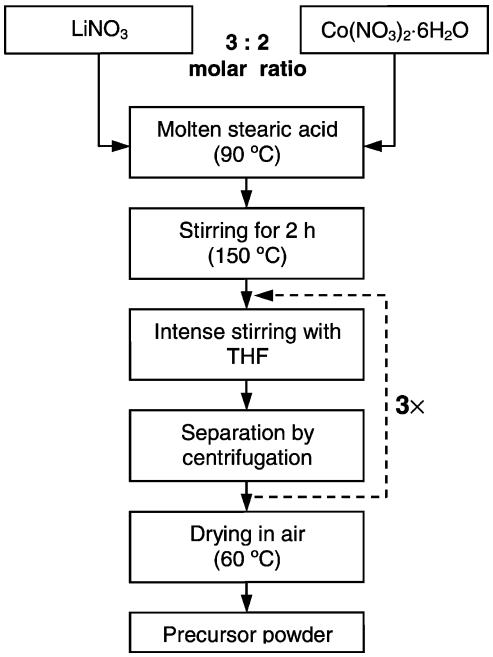

Fig. 1. Illustration of the protocol used in the preparation of emulsion-derived powder.

150 °C for 2 h. Special care is needed in this step because of the eventual formation of flames. The black powder obtained after the stirring step was then submitted to mechanical stirring with tetrahydrofuran (THF) solvent and then the solution was centrifuged (9000 rpm) for 15 min. The micro-precipitate obtained, i.e. the emulsion-derived precursor, was then dried at 60 °C in air to evaporate the THF solvent. The resulting emulsion-derived powders were gray in color and physically similar to starch. In this paper, we will denote the emulsion-derived powder prepared with molar proportion metal/acid 1:1 and 2:1 as E1- and E2-emulsion, respectively.

The FTIR spectra of E2- and E1-emulsions were collected using a Nicolet 5ZDX spectrometer (KBr beam splitter, 64 scans, range 400–4000 cm^{-1}, resolution 2 cm^{-1}). Thermogravimetric/differential thermal analysis (TGA/DTA) of the E1-emulsion precursor was performed in synthetic air (heating rate 10 °C min^{-1}) using a TA Instruments (model SDT-2960 Simultaneous Analyser). Every X-ray diffraction (XRD) pattern shown in this paper was collected using a SIEMENS D5005 diffractometer (Cu Kα radiation, graphite monochromator, range 10–90°, steps of 0.02°, 8 s per step). The specific surface area was measured by the Brunauer–Emmett–Teller (BET) method with N_2 (Quantachrome-NOVA 1200). The scanning electron microscope was a JEOL-JSM 5200. The grain size distribution of $LiCoO_2$ obtained from the E1-emulsion and used in the preparation of composite electrode was determined by a particle size analyzer (Mastersize 2000, Fraunhofer diffraction).

The electrochemical characterization was carried out using Swagelock-type cells assembled with two separators (Celgard®-2400) soaked with electrolyte $LiPF_6$, 1 mol l^{-1} in a 1:1:3 (w/w) solution of propylene carbonate (PC), diethylene carbonate (DEC) and dimethyl carbonate (DMC)-(all Selectipur grade). The reference and auxiliary electrodes were metallic lithium. Charge/discharge cycles at room temperature were performed using a Mac-Pile cycler and the cells were assembled in a dry-box.

The composite electrodes studied were disks with 8 mm diameter. They were prepared by spreading a slurry of active oxide material (67 wt.%), polyvinylidene fluoride binder (PVDF, Solvay, 12 wt.%), carbon (Keitjen Black, 18 wt.%), graphite (Fluka, 400 mesh 3 wt.%) and acetone on Al foil (thickness 60 μm) using a Doctor-blade in air. The graphite was used to provided a better mechanical stability of active membrane deposited on Al substrate. The composite foil was also hot pressed (1.0×10^7 Pa, 100 °C) for better electric contact between the Al foil and the membrane electrode and finally the electrode disks were purged under vacuum at 120 °C for 24 h. The $LiCoO_2$ used in the preparation of composite electrode was obtained from E1-emulsion (calcination at 700 °C for 6 h in air, alumina crucible). This $LiCoO_2$ powder was rinsed with deionized H_2O and submitted to ultrasonic treatment to remove lithium carbonate traces.

3. Results and discussion

3.1. $LiCoO_2$ synthesis

Fig. 2 shows the FTIR spectra and the XRD patterns collected for the E1- and E2-emulsion-derived powder, respectively. In short, both FTIR spectra (left Fig. 2) have bands from 500 to 700 cm^{-1} that can be assigned to the Co–O vibrations, while the band at 3417 cm^{-1} can be ascribed to the stretching of –OOH group. The strong bands at 2880 cm^{-1} are due to the stretching of aliphatic chain (–CH), and the strong bands near 1500 cm^{-1} are assigned to nitrate ions ($–NO_3^-$). The small band at 1717 cm^{-1} corresponds to the –COOH group vibration of residual stearic acid. The FTIR spectra of both emulsion-derived powders present intense bands at 1578 and 1554 cm^{-1} that are assigned to lithium stearate. The Fig. 2 (right) shows also that E1-emulsion XRD pattern are associated with $CH_3(CH_2)_{16}COOLi$ and CoOOH, while the E2-emulsion pattern reveals that the dominant phases are CoOOH, $CH_3(CH_2)_{16}COOLi$ and CoO.

Therefore, the chemical composition of the emulsion-derived powders obtained as described in Fig. 1, depend on the stearic acid concentration used in the preparation. This precursor was found to be rich in CoOOH and $CH_3(CH_2)_{16}COOLi$ only when it was used in the preparation of emulsion with the molar proportion of metal/stearic acid 1:1. For a molar proportion of metal/stearic acid of 2:1, the $CH_3(CH_2)_{16}COOLi$ concentration in the emulsion-derived powder is lower and the dominant phases are CoO and CoOOH. The residual stearic acid, as well as

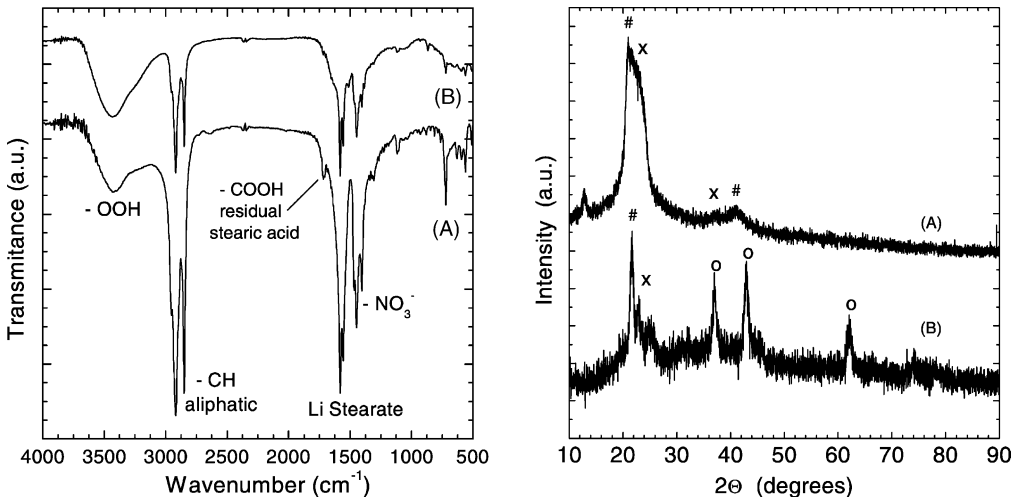

Fig. 2. FTIR spectra and XRD patterns collected for the emulsion-derived powder E1 (A) and E2 (B). The labels represent CoOOH (#), $CH_3(CH_2)_{16}COOLi$ (×), CoO (o) phases.

traces of nitrates, were detected from FTIR spectra in both emulsion-derived powders.

Fig. 3 shows the TGA/DTA curves of the E1-emulsion, where the dominant phases are CoOOH and $CH_3(CH_2)_{16}$ COOLi. The weight loss of the micro-precipitate precursor occurs basically in two steps, at 21–200, 200–550 °C, and terminates at 700 °C. The weight loss and the small endothermic peaks for temperatures lower than 350 °C are associated with the melting of residual stearic acid (∼125 °C), water and THF evaporation. Above 300 °C, the exothermic events detected in Fig. 3 are due to the decomposition of the organic phase, formation of Li_2CO_3 and $LiCoO_2$ phases as are shown in the XRD patterns of Fig. 4. The intense exothermic peak at 522 °C is correlated to the transformation of lithium stearate into lithium carbonate.

Fig. 4 shows the X-ray diffraction patterns of the resulting product of several firings of the E1-emulsion for 6 h at temperatures near those of the more intense exothermic peaks. At 480 °C, occurs the formation of low temperature-$LiCoO_2$ (LT-$LiCoO_2$) with cationic disorder and the formation of Li_2CO_3. The next exothermic peaks appear associated with the reduction of the disordered phase LT-$LiCoO_2$ and the increasing of a well-ordered $LiCoO_2$ phase (T ∼520 °C). The Bragg intensity of the (0 0 3) line increases and complete splitting between the (0 0 6)/(1 0 2) and (1 0 8)/(1 1 0) Bragg peaks (Fig. 4) occurs which confirms this phase transition. The $CH_3(CH_2)_{16}COOLi$ and CoOOH micro-precipitate acts thus very well as a template for the formation of well-ordered $LiCoO_2$, because at 550 °C (the exothermic

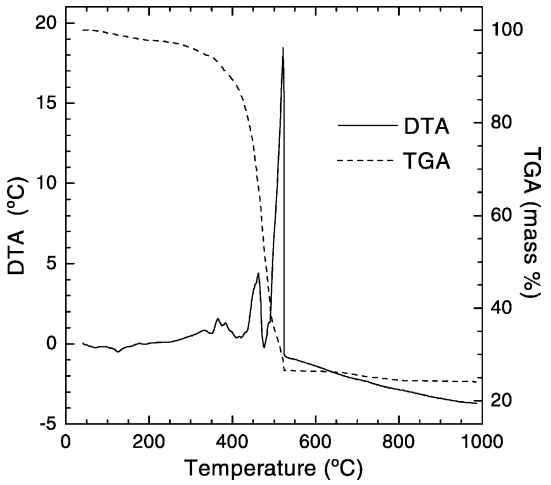

Fig. 3. TG/DTA curves for E1-emulsion-derived precursor composed mainly by CoOOH, $CH_3(CH_2)_{16}COOLi$ and residual stearic acid.

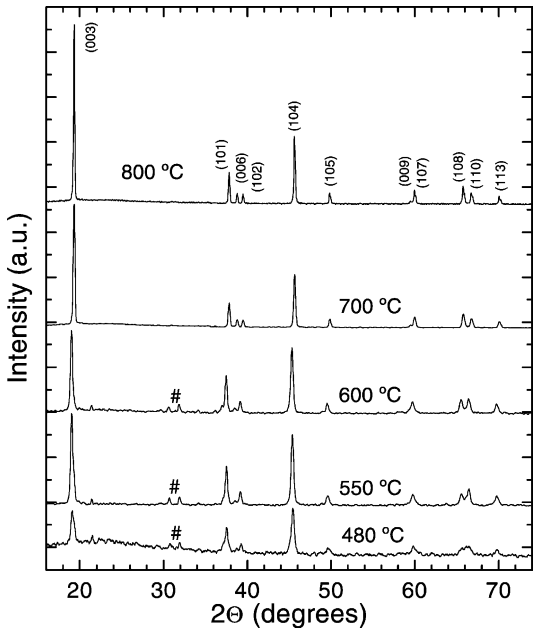

Fig. 4. (A) XRD patterns collected for the E1-emulsion-derived powder submitted to successive heating in air (rate 5 °C/min, 3 h for each heating). Label (#) indicates the Li_2CO_3 phase.

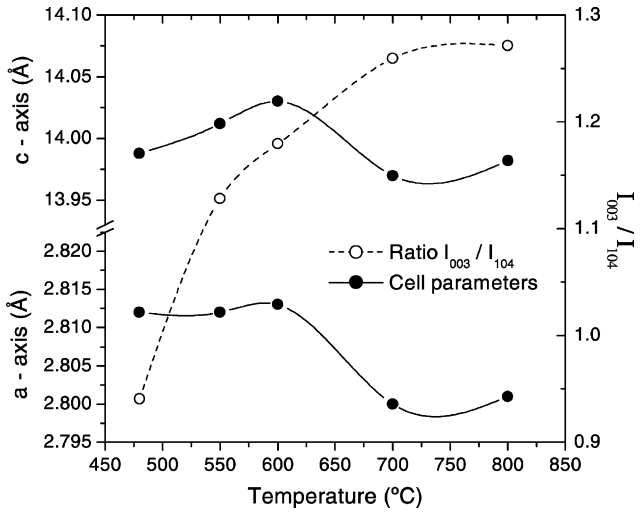

Fig. 5. Evolution of cell parameters of the hexagonal $LiCoO_2$ phase and Bragg intensity ratio I_{003}/I_{004} obtained from Fig. 4.

peak most intense in Fig. 3) we have a $LiCoO_2$ with a small cationic disorder. Fig. 5 shows the cell parameters and Bragg intensity ratio I_{003}/I_{004} associated with cationic disorder as a function of the calcination temperature of the precursor mixture, supports this phase transition. For temperatures above 480 °C, the $LiCoO_2$ oxide obtained is the hexagonal structure (*R*-3*m*) and it becomes quite ordered at 800 °C as is indicated by the ratio of the cell parameters (Fig. 5).

The microstructure of $LiCoO_2$ calcined at 800 °C using the two kinds of emulsions are shown in Fig. 6. When the

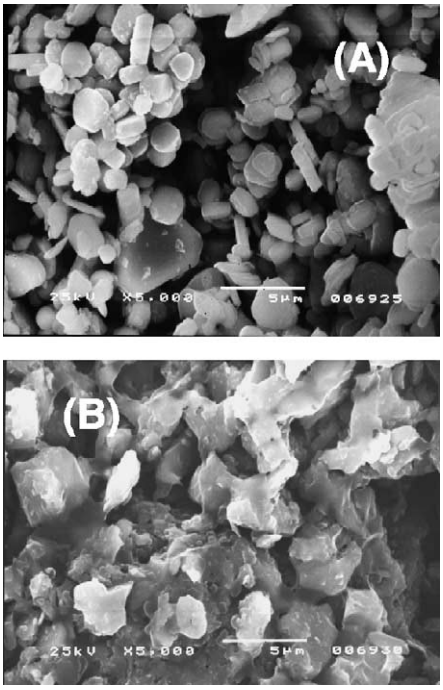

Fig. 6. SEM micrography of the $LiCoO_2$ powder from E1-emulsion (A) and E2-emulsion both calcined at 800 °C in air.

E1-emulsion was used to obtain the well-ordered $LiCoO_2$, their particles were found crystallized as quasi-hexagonal pellets (Fig. 6A), while the use of E2-emulsion yielded $LiCoO_2$ powder that is composed of huge aggregates of particles with an irregular shape (Fig. 6B). The specific surface areas of the $LiCoO_2$ powders were 7.4 and 1.1 $m^2\,g^{-1}$, respectively, values that are consistent with the morphology observed in Fig. 6A and B. For the $LiCoO_2$ powder obtained from the E1-emulsion, there was also a very narrow grain size distribution ($d_{10} = 0.31$, $d_{50} = 3.14$, $d_{90} = 6.30\,\mu m$).

Micro-precipitation in molten stearic acid appears to be an interesting method of preparation of $LiCoO_2$, mainly when the concentration of stearic acid is sufficient to form $CH_3(CH_2)_{16}COOLi$ and CoO is absent. The lithium stearate and CoOOH are therefore adequate reagents to form $LiCoO_2$ with uniform particles and a high specific surface area. When the lithium stearate concentration is very low and the precursor is rich in CoO (E2-emulsion), the calcination of emulsion-derived powder at 800 °C by 6 h in air, led also to formation of well-ordered $LiCoO_2$ (*R*-3*m*), but the resulting powder presented grains that are composed by huge aggregate particles of irregular shape.

Finally, it must be mentioned that the E1 and E2 emulsion-derived powders have a hydrophobic character. This is an interesting behavior because it suggests that the cobalt and lithium salts may be encapsulated by the organic phase detected in the FTIR spectra (Fig. 2), e.g. the residual stearic acid. The excess of stearic acid should be beneficial and it is reasonable to expect that it plays a role in the morphology of $LiCoO_2$ particles (*R*-3*m*). The THF rinse of emulsion-derived powder could thus be eliminated in Fig. 1.

3.2. Electrochemical characterization

Fig. 7 shows the galvanostatic charge/discharge cycles of a composite electrode prepared with the $LiCoO_2$ powder shown in Fig. 6A. All $LiCoO_2$ electrodes reach a specific capacity in the first charge of over 150 $mAh\,g^{-1}$ and irreversibility in deinsertion/insertion reaction. The $LiCoO_2$ electrodes still have a capacity fade that increases with increase of current density.

The nominal lithium quantity extracted from $LiCoO_2$ during the first discharge is about 0.6 mol. This deinsertion implies structural alterations [28,29] that can reduce the lithium intercalation kinetics. In fact, for $x > 0.5$ in Li_xCoO_2 there is a reduction in the lithium chemical diffusion coefficient, beside the metallic behavior observed for $LiCoO_2$ [30]. When *x* is over 0.5 mol there occurs a large increase in the volume of the hexagonal phase of $LiCoO_2$. For example, the volume of unitary cell V_{cell} that is 14.066 $Å^3$ for $x = 1$ expands to 14.437 $Å^3$ for $x = 0.37$, while for $x = 0.53$ the increase of V_{cell} is smaller, i.e. only 12.8% of initial volume in the Li_xCoO_2 [6]. Fig. 7 shows that increasing capacity fade should be associated with a poor electronic conductivity of the electrode. This is evident when the rate

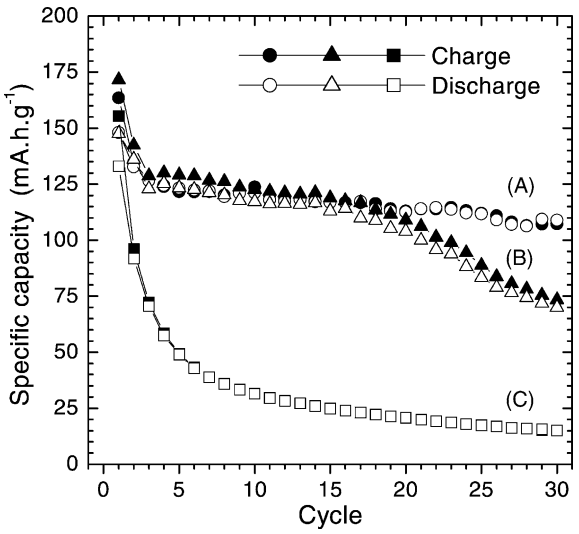

Fig. 7. Specific capacity of $LiCoO_2$ composite electrodes prepared with powder shown in Fig 6A. The charge/discharge currents and rates were 100 μA, ∼*C*/15 (A); 200 μA, ∼*C*/8 (B); and 400 μA, ∼*C*/3 (C). For all electrodes, the current density was ∼10 mA g^{-1} and the potential cut-off limit was 2.6–4.35 V vs. Li/Li^+.

of charge/discharge of the electrode is large as in Fig. 7C (rate of charge/discharge ∼*C*/3). The long life specific capacity observed in Fig. 7A (∼110 mAh g^{-1}) is therefore a good result if we consider the value reached by the specific capacity in the first deinsertion (∼150 mAh g^{-1}).

These electrochemical results suggest that the morphology of $LiCoO_2$ obtained by the micro-precipitation method (Fig. 6A) permits the preparation of composite electrodes that support well the stress that can otherwise damage the grains and affect the electrical contact between particles and the composite-electrode-current collector (i.e. stress provoked by large variation in volume of particles for $x \sim 0.4$ and charging/discharging of electric double layer in the interface of particles) [1,2].

4. Conclusions

The present work describes a new method to preparation of oxides using micro-precipitation in molten stearic acid. The temperature of formation of ordered $LiCoO_2$ (*R*-3*m*) (700 °C) is similar to that which has been found by Amatucci et al. [31] in the hydrothermic synthesis that is an interesting method for large scale production. The micro-precipitate method proposed in this work yields nice particles, as for the hydrothermic method, but the elimination of nitrate occurs during the self preparation of the emulsion (by reaction between nitrates and stearic acid). The micro-precipitation in molten stearic acid may be used easily on a large scale. However, during the reaction of nitrates with stearic acid, we recommend care. The burning of the stearic acid generates only CO_2 and H_2O.

This novel emulsion method applied to $LiCoO_2$ yields a polycrystalline compound at 800 °C with a narrow grain sub-micron size distribution, high specific surface area (d_{10} = 0.31, d_{50} = 3.14, d_{90} = 6.30 μm, 7.4 $m^2\ g^{-1}$) and particles with a uniform shape (quasi-hexagonal). The method of micro-precipitation in molten stearic acid is an interesting route to preparation of $LiCoO_2$ that can be extended to other oxides used in Li-ion batteries.

Acknowledgements

We thank FAPESP, CAPES for L.A. Montoro's and S.M. Lala's Ph.D. fellowships, CNPq (301493/95-2) and J.A. Maulin of FMRP to technical support with the scanning electron microscope.

References

[1] H. Wang, Y.-H. Jang, B. Huang, D.R. Sadoway, Y.-M. Chiang, J. Electrochem. Soc. 146 (1999) 473.
[2] J.M. Rosolen, F. Decker, J. Electrochem. Soc. 143 (1996) 2417.
[3] G.G. Amatucci, J.M. Tarascon, L.C. Klein, J. Electrochem. Soc. 143 (1996) 1143.
[4] T. Ohzuku, A. Ueda, J. Electrochem. Soc. 141 (1994) 2972.
[5] T. Ohzuku, A. Ueda, N. Nagayama, Y. Iwakoshi, H. Komori, Electrochim. Acta 38 (1993) 159.
[6] J.M. Rosolen, P. Ballirano, M. Berrettoni, F. Decker, M. Gregorkiewitz, Ionics 4 (1997) 345.
[7] H. Chen, X. Qiu, W. Zhu, P. Hagenmuller, Electrochem. Commun. 4 (2002) 488.
[8] D. Caurant, N. Baffier, B. Garcia, J.P. Pereira-Ramos, Solid State Ionics 91 (1996) 45.
[9] T. Takada, H. Hayakawa, E. Akiba, F. Izumi, B.C. Chakoumakos, J. Power Sources 68 (1997) 613.
[10] Y. Fujita, K. Amine, J. Maruta, H. Yasuda, J. Power Sources 68 (1997) 126.
[11] G.T.K. Fey, K.S. Chen, B.J. Hwang, Y.L. Lin, J. Power Sources 68 (1997) 519.
[12] Y.-M. Chiang, Y.-I. Jang, H. Wang, B. Huang, D.R. Sadoway, P. Ye, J. Electrochem. Soc. 145 (1998) 887.
[13] R.J. Gummow, D.C. Liles, M.M. Thackeray, Mater. Res. Bull. 28 (1993) 1177.
[14] T.M.T.N. Tennakoon, G. Lindbergh, B. Bergman, J. Electrochem. Soc. 144 (1997) 2296.
[15] P.N. Kumta, D. Gallet, A. Waghray, G.E. Blomgren, M.P. Setter, J. Power Sources 72 (1998) 91.
[16] D. Larcher, M.R. Palacin, G.G. Amatucci, J.M. Tarascon, J. Electrochem. Soc. 144 (1997) 408.
[17] C.H. Chen, E.M. Kelder, M.J.G. Jak, J. Schoonman, Solid State Ionics 86 (1996) 1301.
[18] Z.S. Peng, C.R. Wan, C.Y. Jiang, J. Power Sources 72 (1998) 215.
[19] G.G. Amatucci, J.M. Tarascon, D. Larcher, L.C. Klein, Solid State Ionics 84 (1996) 169.
[20] B. Garcia, J. Farcy, J.P. Pereira-Ramos, J. Perichon, N. Baffier, J. Power Sources 54 (1995) 373.
[21] P.N. Kumta, D. Gallet, A. Waghray, G.E. Blomgren, M.P. Setter, J. Power Sources 72 (1998) 91.
[22] C.Y. Kuo, Solid State Technol. 17 (1974) 49.
[23] P. Kalyani, N. Kalaiselvi, N. Muniyandi, J. Power Sources 11 (2002) 232.

[24] W.T. Jeong, K.S. Lee, J. Power Sources 104 (2002) 195.
[25] S.K. Chang, H.-J. Kweon, B.K. Kim, D.Y. Jung, Y.U. Kwon, J. Power Sources 104 (2002) 125.
[26] M.A. López-Quintela, J. Rivas, J. Colloid Interface Sci. 158 (1993) 446.
[27] S.M. Lala, E. di Donatti, L.A. Montoro, J.M. Rosolen, J. Power Sources 114 (2003) 127.
[28] L.A. Montoro, M. Abbate, J.M. Rosolen, Electrochem. Solid State Lett. 3 (2000) 416.
[29] L.A. Montoro, M. Abbate, E.C. Almeida, J.M. Rosolen, Chem. Phys. Lett. 309 (1999) 14.
[30] J.M. Rosolen, F. Decker, J. Electroanal. Chem. 501 (2001) 253.
[31] G.G. Amatucci, J.M. Tarascon, L.C. Klein, Solid State Ionics 84 (1996) 169.